GDC-Based Low-Temperature SOFCs Powered by Hydrocarbon Fuels

Shaowu Zha, Ashley Moore, Harry Abernathy, and Meilin Liu*,z

School of Materials Science and Engineering, Georgia Institute of Technology, Atlanta, Georgia 30332-0245, USA

The critical issues facing the development of economically competitive solid oxide fuel cell (SOFC) systems include lowering the operation temperature and creating novel anode materials and microstructures capable of efficiently utilizing hydrocarbon fuels. In this paper, we report our recent progress in developing more efficient anodes for direct utilization of methane and propane in low-temperature SOFCs. Anode-supported SOFCs with an electrolyte of 20 μm thick Gd-doped ceria (GDC) were fabricated by copressing, and both Ni- and Cu-based anodes were prepared by a solution impregnation process. Results indicate that both microstructure and composition of the anodes, as fabricated using a solution impregnation technique, greatly influence fuel cell performance. At 600°C, SOFCs fueled with humidified H_2, methane, and propane reach peak power densities of 602, 519, and 433 mW/cm^2, respectively.
© 2004 The Electrochemical Society. [DOI: 10.1149/1.1764566] All rights reserved.

Solid oxide fuel cells (SOFCs) have received great attention in the past 20 years due to their potential for providing a highly efficient and environmentally benign way of generating electricity.[1-3] However, several obstacles still remain to be overcome before SOFCs are economically competitive in the marketplace. While some research focuses on the development of SOFCs for operation at high temperatures of 900-1000°C, it has become increasingly important to reduce the operation temperature of the fuel cells to below 800°C in order to substantially increase the life of SOFCs; widen the selection of electrodes, interconnect, and manifold materials; and reduce the cost of material processing and cell fabrication. Two approaches are widely employed to lower the resistance of dense electrolyte membranes at lower operating temperatures: decreasing the traditional yttria-stabilized zirconia (YSZ) (8 mol % Y_2O_3-ZrO_2) electrolyte thickness,[4,5] or using alternative materials of higher ionic conductivity at lower temperatures. In our previous work, SOFCs with thin doped-ceria electrolyte demonstrated that they can operate at temperatures as low as 400°C when using H_2 as the fuel.[6,7]

Another challenging issue is to operate SOFCs on hydrocarbon fuels. Internal steam reforming is a typical approach. A steam-to-carbon ratio of >2:1 is often used to prevent carbon deposits at the anode. Apparently, however, this method will introduce larger operation cost and yield lower energy efficiency to the whole fuel cell system. A more promising way of directly using hydrocarbon fuels has recently surfaced. Carbon deposits were suppressed by using anode compositions that do not catalyze coking of hydrocarbon, especially running SOFCs at relatively low temperatures. Cu-ceria/doped ceria is found to be one possible anode material used for direct utilization of hydrocarbon fuels in SOFCs,[8,9] because it is relatively inert to hydrocarbon reactions, particularly coking, compared to Ni. SOFCs operating in this way at reduced temperatures (<800°C) provide useful power densities with hydrocarbon fuels without addition of significant amount of steam, CO_2, or O_2.[5,8,10] However, Cu or CuO has a low melting point that makes it difficult to apply conventional ceramic processing methods to fabricate Cu-containing SOFCs.[9]

In this paper, we report our recent progress in development of new anode materials for direct utilization of methane and propane in low-temperature SOFCs. Anode-supported SOFCs with a 20 μm Gd-doped ceria (GDC) electrolyte were fabricated by copressing, and both Ni- and Cu-based anodes are prepared by a solution impregnation process. The solution impregnation fabrication technique, as well as the effect of microstructure and composition of the anode materials on fuel cell performance, is also discussed.

Experimental

Two types of anode-supported fuel cells are fabricated by copressing and by a combination method of copressing and metallic-ion impregnation. In the copressing method, the nickel oxide and GDC ($Ce_{0.9}Gd_{0.1}O_{1.95}$) powders were prepared using a glycine-nitrate process as described elsewhere.[11] After combustion, they were calcined at 850 and 600°C for 5 and 2 h, respectively, to form completely pure cubic phases. The GDC powder has a foamed structure with extremely low-tapped density, which is always used for dry-pressing of thin electrolyte films in this study. The powder was added to a metal die in which NiO and GDC composite powder with weight ratio of 65-35 was prepressed under 200 MPa as substrate. The two layers of GDC and substrate were then copressed at 250 MPa to form a green bilayer and subsequently cofired at 1350°C in air for 5 h to densify the GDC film. The electrolyte film thickness can be easily controlled with the amount of GDC foamy powder. A slurry consisting of 70 wt % $Sm_{0.5}Sr_{0.5}CoO_3$ (SSC, Rhodia), 30 wt % GDC, and V-006 binder (Heraeus) was applied to the surface of the electrolyte by screen-printing, and then fired at 1000°C in air for 2 h to form a porous cathode on the single cell. The effective area of the fuel cell is ∼0.25 cm^2. The fabrication of cathodes for all cells
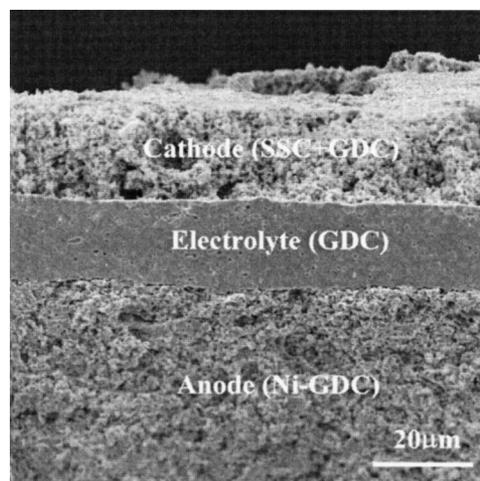

Figure 1. A cross-sectional view (SEM photograph) of a Ni-GDC anode-supported SOFC with a thin GDC electrolyte layer.

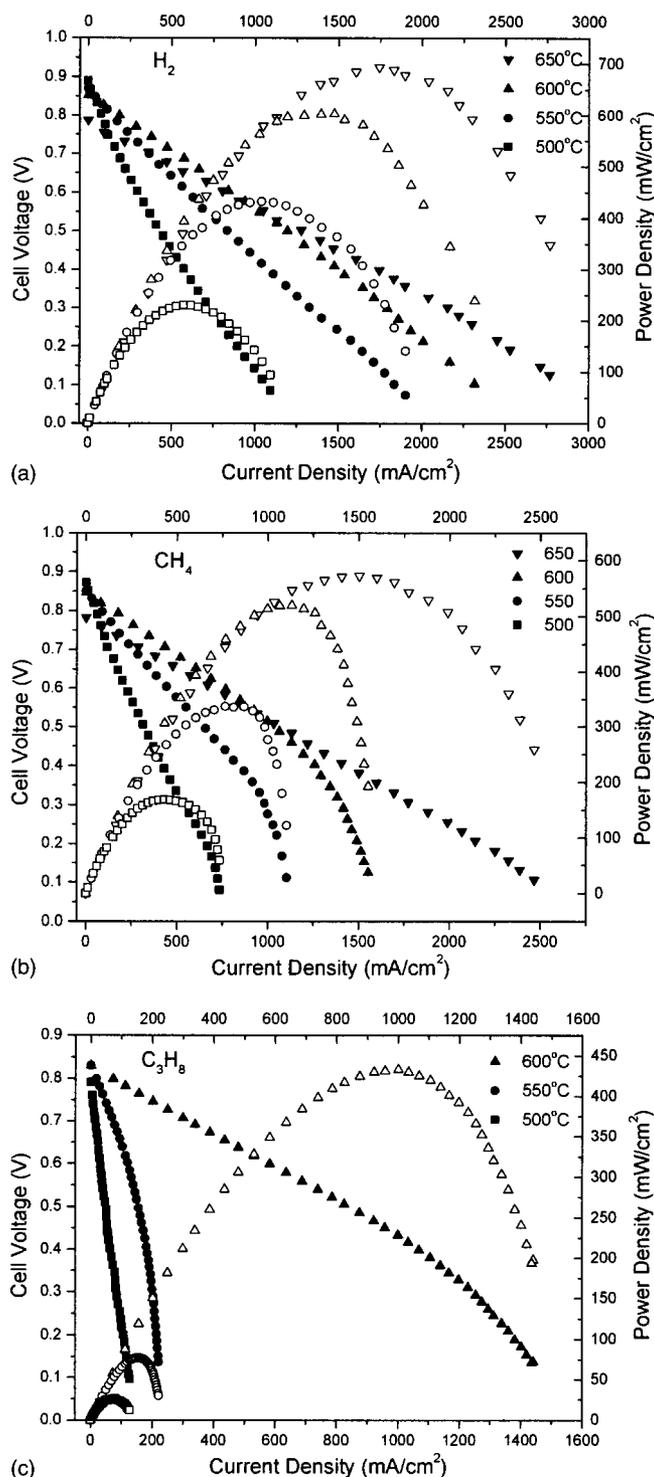* Electrochemical Society Active Member.
z E-mail: meilin.liu@mse.gatech.edu

Figure 2. Cell voltages and power densities as a function of current density for a cell with Ni-GDC anode fabricated by copressing operated at different temperatures (500-650°C) with different fuels: (a) H_2, (b) CH_4, and (c) C_3H_8 as the fuel gas.

Table I. Typical fuel cell performance.

Temperature (°C)	H_2		CH_4		C_3H_8	
	OCV	P_{max}	OCV	P_{max}	OCV	P_{max}
500	0.889	230	0.872	169	0.791	27
550	0.869	432	0.850	336	0.830	77
600	0.852	602	0.846	519	0.830	433
650	0.787	694	0.782	572	···	···

Unit of open-circuit potential (OCV): V; maximum power density (P_{max}): mW/cm^2.

ties of the precursors, cerium nitrate and gadolinium nitrate, were dissolved separately in water, mixed, and coprecipitated with dilute oxalic acid solution, which was adjusted to neutral pH (6.6-6.9) by adding ammonia solution throughout the reaction. The concentration of oxalic acid and Ce^{3+}/Gd^{3+} mixed solution was 0.3 mol/L. The resulting precipitate was vacuum-filtered, washed five times with water and ethanol, respectively, and dried at 50°C in an oven. After firing at 750°C, the oxide powders were confirmed by X-ray diffraction analysis (XRD, Phillips PW-1800) to be single phase of fluorite structure. This coprecipitation-derived GDC is hereafter abbreviated as C-GDC. The C-GDC and rice-starch powders were weighed in an appropriate ratio and mixed in a mortar gently before being cold-pressed as substrate. Then a small amount of foamy GDC powder was added and copressed, as described previously. The green bilayer pellets were then cofired at 1350°C in air for 5 h to obtain dense electrolyte film and sponge-like structured GDC matrix. This porous matrix assumed as cell anode was impregnated with 3 mol/L
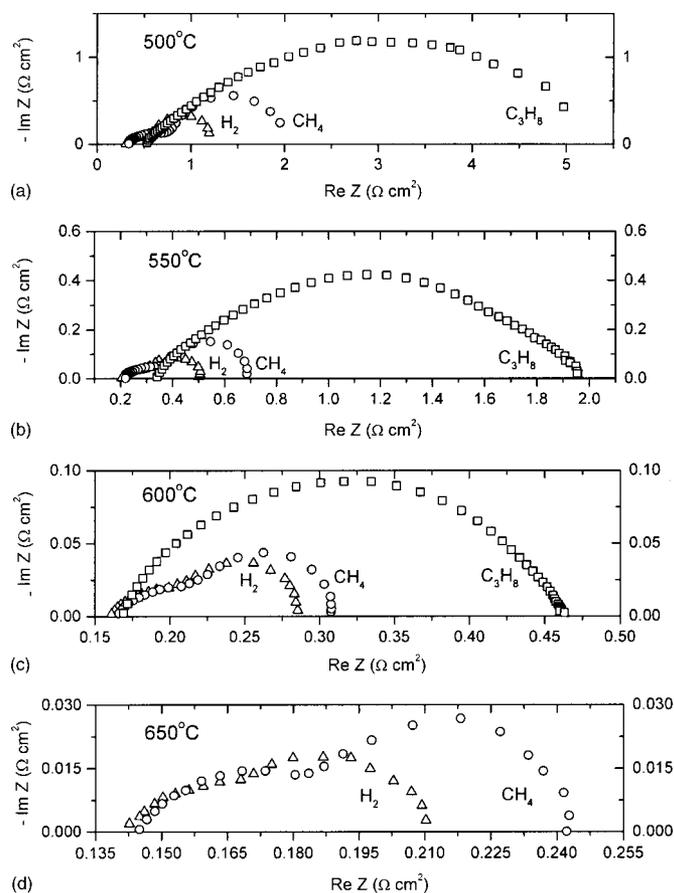

Figure 3. Impedance spectra measured between 500 and 650°C at OCV for humidified H_2, CH_4, and C_3H_8 fuels.

(including the symmetrical cells) tested in this study was kept as consistent as possible so that the cathodic polarization resistances of all cells were relatively constant.

A novel ion-impregnation approach was also developed to make anode-supported fuel cells with Cu-GDC based anode structure and GDC thin electrolyte film. Coarse GDC powder was synthesized using an oxalate coprecipitation route.[12,13] The appropriate quanti-

Table II. Resistance (in Ω cm^2) of cell components.

T (°C)	H₂			CH₄			C₃H₈		
	R_b	R_p	R_a	R_b	R_p	R_a	R_b	R_p	R_a
500	0.306	1.146	0.136	0.323	2.202	1.192	0.513	6.892	5.882
550	0.204	0.405	0.045	0.218	0.637	0.277	0.336	2.203	1.843
600	0.160	0.175	0.025	0.165	0.202	0.052	0.169	0.410	0.260
650	0.141	0.112	0.022	0.145	0.155	0.065	⋯	⋯	⋯

$Cu(NO_3)_2 \cdot 6H_2O$ (99.9%, Aldrich) solution, dried in air, and calcined to 900°C to decompose the nitrate ions and form copper oxide. The impregnation, drying, and calcination processes were repeated 8-10 times before appropriate amount of CuO was achieved. CuO was reduced to Cu *in situ* when the fuel cell was run on reducing fuel gas. 70 wt % SSC and 30 wt % GDC was applied as cathode. This combination method of copressing and metallic-ion impregnation was also used to fabricate thin electrolyte-based fuel cells with a Ni-GDC structured anode.

XRD was used to analyze the Cu impregnation process. The morphologies of the powders and anode were observed by a scanning electron microscope (SEM, Hitachi S-800) before and after impregnation. The Raman spectra were acquired at room temperature under ambient conditions, using a backscattering geometry on a Renishaw Raman System 2000 spectrometer to detect the carbon deposits when hydrocarbon gases were applied as fuels.

For the electrochemical measurements, the two-electrode pellets were mounted in a two-lead (Ag) two-electrode setup. Ag paste (Heraeous C4400UF) was used to seal the anode compartment and also acted as electrical contact between anode and silver wire. Electrochemical characterizations were performed at temperatures from 500 to 650°C under ambient pressure. Fuel cell performances were measured with a Solarton 1287 interfaced with a computer. Stationary air was fed as oxidant, and humidified methane and propane (3 vol % H_2O) as fuels. Humidified hydrogen was also fed as fuel for comparison. The impedance was measured typically in the frequency range from 0.01 Hz to 100 kHz using an EG&G lock-in amplifier (model 5210) and an EG&G potentiostat/galvanostat (model 273A) interfaced with a computer.

Results and Discussion

Ni-GDC supported SOFC fabricated by copressing.—Figure 1 displays a typical cross-sectional micrograph of a Ni-GDC anode-supported SOFC with a thin GDC electrolyte layer. This micrograph
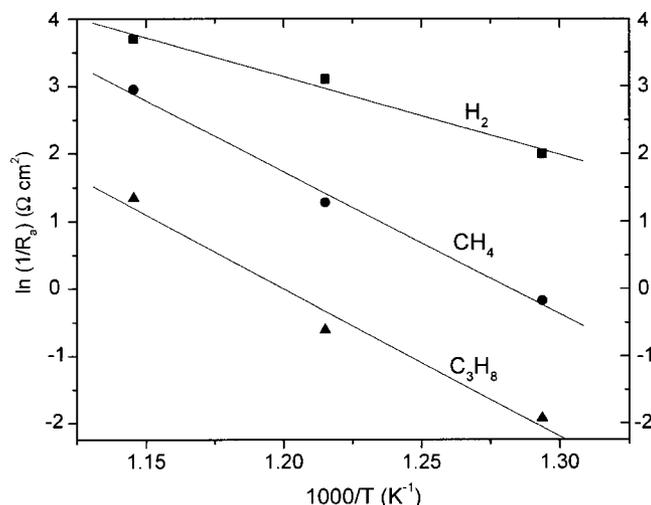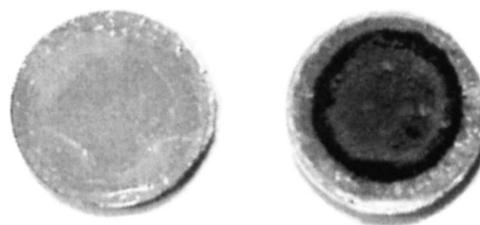

Figure 5. Photograph of the surface of Ni-GDC anodes running (left) on methane for 50 h and (right) propane for 3 h at 600°C.

shows a dense, 20 µm thin GDC electrolyte sandwiched between the porous anode and cathode layers. The electrolyte film thickness can be controlled during copressing with the amount of GDC foamy powder synthesized by a glycine-nitrate process, due to its rather low-tapped density.

The performance was measured at temperatures between 500 and 650°C, including current-voltage curves and impedance spectra of a single cell with the Ni-GDC anode. Three kinds of fuels, hydrogen, methane, and propane, are fed in turn. In the first run, hydrogen flows into the anode chamber and the cell performance was measured from elevated temperature to lower temperature. The cell was subsequently heated again to start the second and third measurement procedure for methane and propane. Figure 2 shows the cell voltage and power density as a function of current density for the three fuels. Table I summarizes some performance data, such as open circuit voltage (OCV) and maximum power density. Extremely high power densities were obtained when hydrogen and methane were used as fuels at operating temperatures below 650°C. For example, the maximum power densities are 602 and 519 mW/cm^2 with OCVs of 0.852 and 0.846 V at 600°C for hydrogen and methane, respectively. To our knowledge, these are the highest performances re-
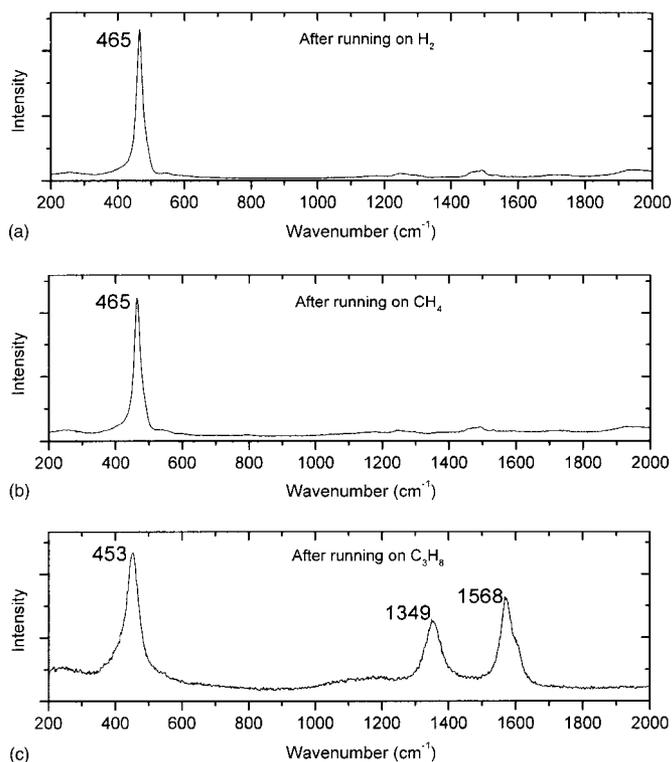

Figure 4. Arrhenius plots of anode/electrolyte interfacial resistances for single cells with different fuels.

Figure 6. Room-temperature Raman spectra of Ni-GDC anode surfaces after running fuel cells on H_2, CH_4, and C_3H_8 fuels for 140, 50, and 3 h at 600°C, respectively.
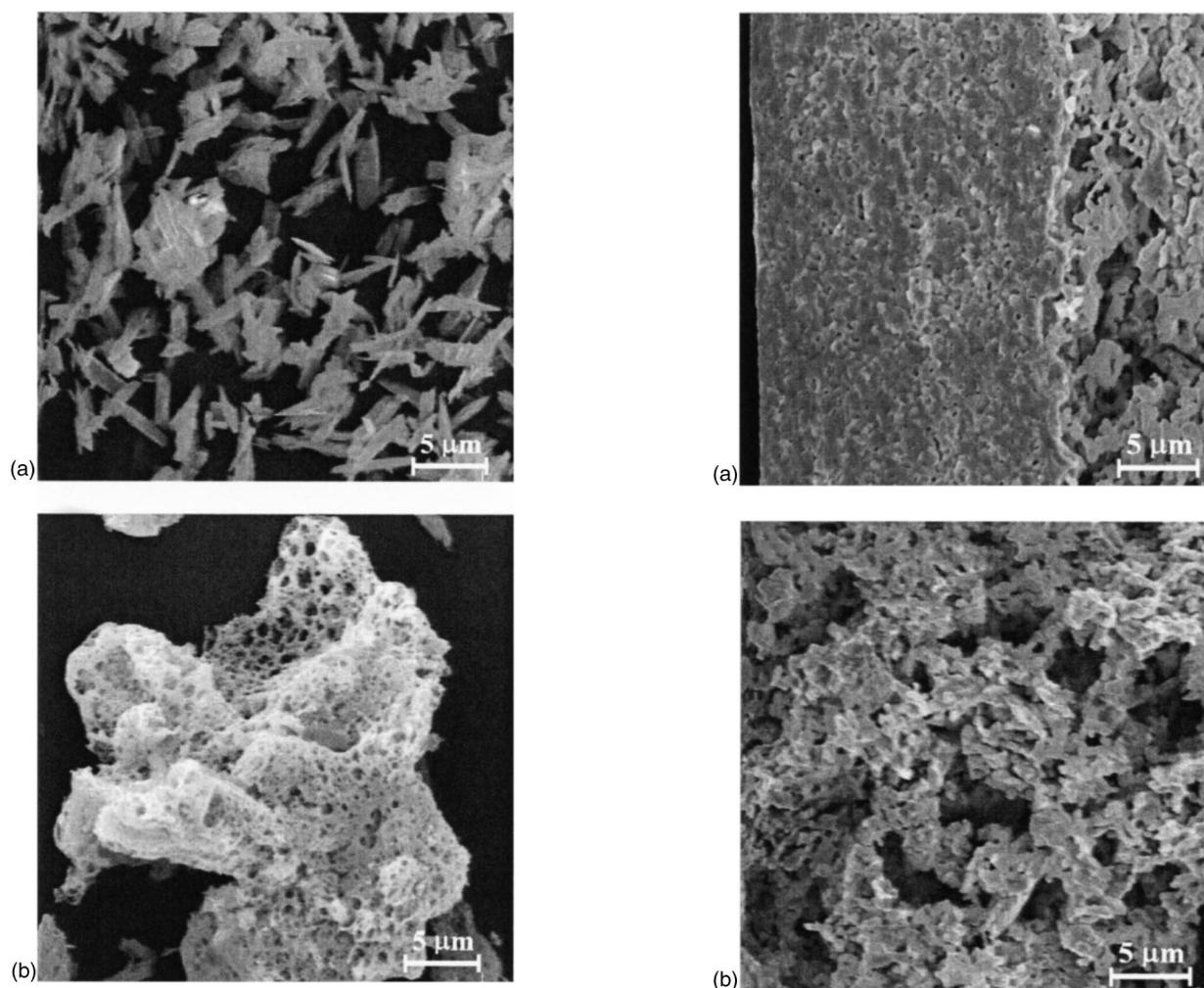
Figure 7. Morphologies of GDC powders synthesized by (a) an oxalic acid coprecipitation (coarse) and (b) a glycine-nitrate combustion (foamy) process after firing at 750°C for 1 h and 600°C for 2 h, respectively.

ported so far for an SOFC operating at such a low temperature, and applying both hydrogen and methane directly as fuels. At all measuring temperatures, the OCV when using methane as fuel is a little lower than that of using hydrogen, while the maximum power density for methane is about 20% lower than for hydrogen. This may be due to the different catalytic activity of Ni toward hydrogen and methane. When using methane, the cell shows apparent concentration polarization at higher current density, in contrast with applying hydrogen, especially when the operation temperature goes down as clearly shown in Fig. 2b. The cell exhibits a quite different performance compared to hydrogen and methane when using propane fuel. The cell achieves a maximum power density of 433 mW/cm^2 with OCV value of 0.830 V for propane at 600°C; however, the electrical output drops dramatically with a decrease in operating temperature. For example, at 550°C the peak power density reduces to only 77 mW/cm^2, compared to 336 mW/cm^2 of methane for the same fuel cell.

Impedance spectroscopy was used to characterize the variation of the cell performance with temperature and fuel composition. Figure 3 shows the impedance spectra measured between 500 and 650°C at OCV using a two-probe configuration for humidified H_2, CH_4, and C_3H_8 fuels. Because the electronic conduction in GDC is not negligible under the fuel cell conditions, the interfacial resistances (R_p) of the fuel cells based on GDC must be adjusted according to the following equation[14,15]
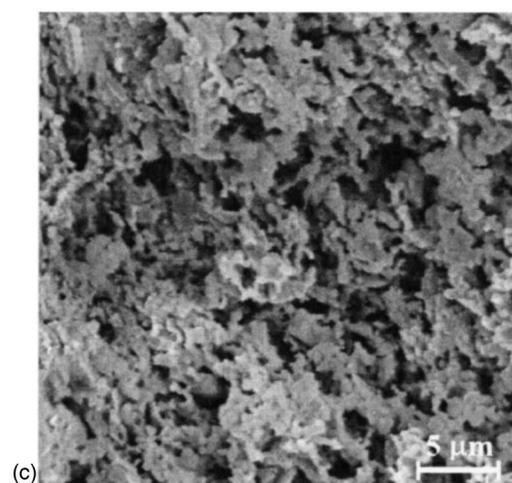

Figure 8. Cross-sectional views (SEM micrographs) of (a) sintered two layers of GDC matrix and dense film, (b) and (c) porous anode structures before and after ion impregnation.

$$R_p = \frac{R_T - R_b}{\dfrac{V_{OC}}{E_N}\left[1 - \dfrac{R_b}{R_T}\left(1 - \dfrac{V_{OC}}{E_N}\right)\right]}$$

where V_{OC} is the open cell voltage, E_N is the Nernst potential across

Table III. Some parameters of the Cu-containing anode fabricated by the impregnation process.

Green porosity before impregnation	65.6%
GDC volume percent in anode matrix	34.4%
Cu volume percent after impregnation and reduction	19.8%
Anode porosity after *in situ* reduction	45.8%

the cell, R_b represents the intercept of the impedance with the real axis at high frequencies, and R_T corresponds to the intercept at the lowest frequencies. To separate anodic impedance R_a from cathodic impedance R_c, a symmetrical cell with SSC-GDC/GDC/SSC-GDC configuration was fabricated and characterized in air using impedance spectroscopy under open-circuit conditions from which the cathode/electrolyte interfacial resistances (R_c) were estimated.[16] Thus, the anode/electrolyte interfacial resistances (R_a) were estimated from

$$R_a = R_p - R_c$$

Table II summarizes the cell resistances between 500 and 650°C for H_2, CH_4, and C_3H_8 fuels. At all temperatures the ohmic resistance (R_b) is almost the same for H_2 or methane; however, the ohmic resistance grows somewhat higher for C_3H_8 as fuel. Similar observations were also reported by Lu *et al.*[17] when H_2 and butane (C_4H_8) were used as the fuel. The anodic interfacial resistance depended greatly on the fuel composition. Especially while operating on propane, the anodic interfacial resistance becomes much higher than both hydrogen and methane. It is reasonable to assume that the cathodic contribution to the overall overpotential was constant because the procedures used for fabrication of all cathodes were kept as consistent as possible. Thus, the different interfacial polarization resistance can be ascribed to the contribution of anode when applying various fuels. When operating on H_2, CH_4, and C_3H_8 fuels at 550°C, R_a is responsible for 11, 43, and 84% of the total interfacial resistance R_p, respectively. As shown in Fig. 3, the shapes of impedance spectra for running on both H_2 and CH_4 fuels are similar, while they are quite different for C_3H_8. Figure 4 presents the Arrhenius plots of anode/electrolyte interfacial polarization resistance *vs.* the reciprocal of absolute temperature. The activation energies determined from the slopes of the lines are 96, 175, and 183 kJ/mol for H_2, CH_4, and C_3H_8 fuels, respectively.

Two cells were operated on methane and propane fuels separately to investigate the carbon deposition with temperature and
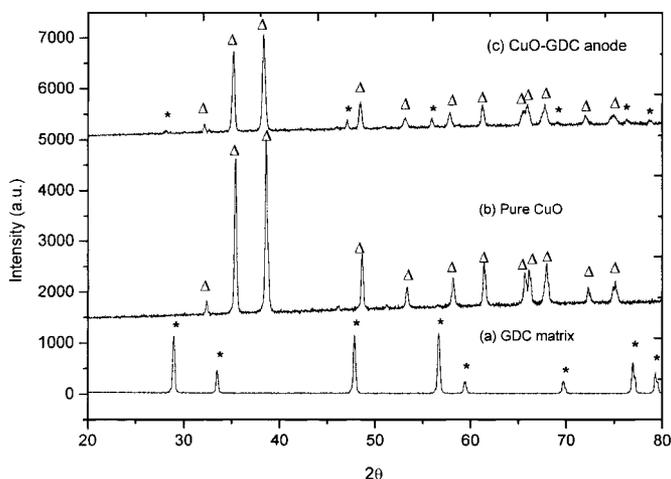

Figure 10. Cell voltage and power density *vs.* current density for a cell with Cu-GDC anode by ion impregnation, measured at 600°C when H_2, CH_4, and C_3H_8 were used as the fuel.

time. In the operating temperature range of 500-650°C, no carbon deposits were visible while running on methane. In contrast, when running on propane at 600°C a large amount of black carbon was deposited on the anode surface after only 3 h, with the results shown in the photographs of Fig. 5. Figure 6 shows the room-temperature Raman spectra of anode surfaces after running fuel cells on H_2, CH_4, and C_3H_8 fuels for 140, 50, and 3 h at 600°C. Figure 6a and b both have an intense F_{2g} mode at about 465 cm^{-1}, which is quite typical for a fluorite-based system like doped ceria.[18] No carbon peak is observed here. However, while operating on propane, two characteristic peaks of amorphous carbon at 1349 (G band) and 1568 cm^{-1} (D band) can be clearly seen in the Raman spectra.[19] The peak wavenumber for fluorite F_{2g} mode also switches from 465 to 453 cm^{-1}. The results indicate that coking of propane occurred on the Ni-GDC anode surface at 600°C. The rate of carbon deposition is larger than that of oxidation in the case of propane, and this causes a buildup of carbon on the surface, which also deactivates the catalytic properties of the anode for fuel oxidation. However, the coking of propane on Ni-GDC anode depends on operating temperature. This can explain why the cell power density decreased sharply with the decrease of operating temperature when propane was used

Figure 9. XRD patterns of (a) GDC matrix, (b) pure CuO, and (c) CuO-GDC anode after CuO impregnation. (*) and (Δ) Indicate doped ceria and CuO peaks, respectively.
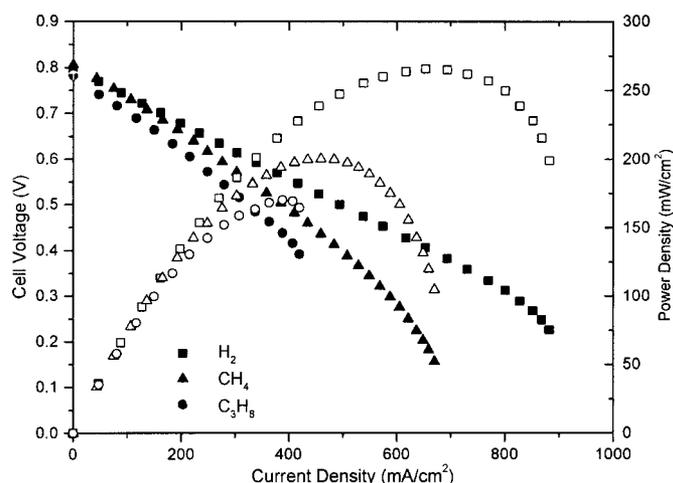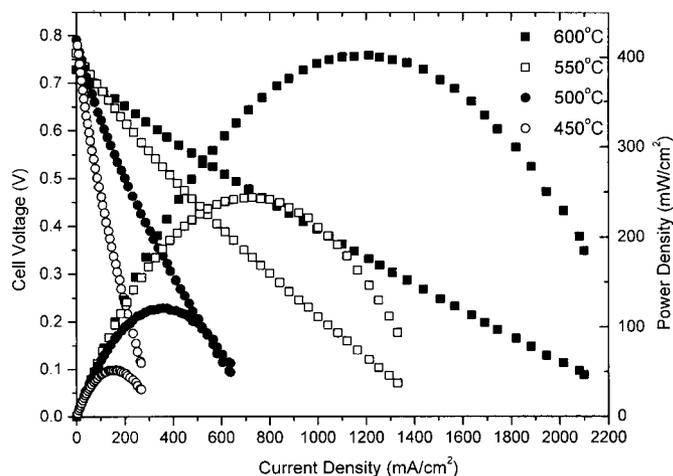

Figure 11. Cell voltage and power density *vs.* current density for a cell with Ni-GDC anode by ion impregnation, running on H_2 at different temperatures (450-600°C).

as the fuel and also why the impedance spectra are quite different from those for hydrogen or methane. In contrast, Ni-GDC anode does not catalyze methane to carbon below 650°C. According to the results of Ref. 8 and 10, direct electrochemical oxidation may be the primary anode reaction for methane, although further investigation is needed to verify it. Thus, methane is a possible hydrocarbon gas that can be used directly as fuel for low-temperature SOFCs based on Ni-GDC anode.

Cu-GDC anode-based SOFC fabricated by copressing and ion-impregnation.—Figure 7 shows the morphologies of coarse GDC (C-GDC) and the foamy GDC (G-GDC) powders synthesized by an oxalic acid coprecipitation and a glycine-nitrate combustion process, respectively. The light and foamy GDC powder was used for the copressed thin electrolyte film, while the coarse C-GDC powder was used for the porous anode substrate. Figure 8a displays the two layers of electrolyte film and porous anode after being fired at 1350°C for 5 h. Figure 8b and c shows the cross-sectional micrographs of porous anode structures before and after ion impregnation. CuO was then reduced *in situ* to Cu when exposed to the fuel before fuel cell tests. By carefully weighing the samples before and after impregnation and calculating the anode volume, the anode porosities and composition proportions are obtained and listed in Table III.

Figure 9 shows the XRD patterns of the anode before and after Cu impregnation. The XRD pattern of pure CuO prepared by firing copper nitrate is also shown for comparison. After ion impregnation all CuO peaks are distinguishable, indicating that CuO was introduced into the sponge-structured GDC anode matrix.

Shown in Fig. 10 are plots of the potential *vs.* current density for an SOFC prepared using a Cu-based anode (Cu-GDC) and a 20 μm thick GDC electrolyte. When H_2, CH_4, and C_3H_8 were used as fuels, the maximum power densities at 600°C achieved 265, 200, and 170 mW/cm^2 with OCVs of 0.796, 0.801, and 0.782 V, respectively. Although both maximum power density and OCV at the same operating temperature are lower than Ni-GDC based SOFCs fabricated by the copressing method discussed in the previous section, no carbon deposition was observed on this Cu-based fuel cell when using propane fuel. Copper can thus be used to replace Ni because it is relatively inert to hydrocarbon reactions, particularly coking. Doped ceria is feasible because of its well-known activity for hydrocarbon oxidation. Nevertheless, great effort is necessary to improve the stability of the cell microstructure and the resulting electrochemical performance for this novel anode-supported SOFC.

Effect of anode microstructure on fuel cell performance.—To investigate the effect of fabrication process and microstructure on fuel cell performance, cells with NiO impregnated in the porous anode matrix were also fabricated. In this case, the procedures used for fabrication of Ni-GDC anodes are identical to those used for Cu-GDC to check the feasibility of so-called combination method of copressing and ion impregnation, although it may not be necessary to prepare Ni-GDC using this approach in practice. Figure 11 presents the performance of one cell operating on hydrogen fuel. The achieved peak power densities were 121, 244, and 402 mW/cm^2 at 500, 550, and 600°C, respectively.

Clearly, these performances are not as good as those for the cells fabricated by copressing, implying that the fabrication process and the resulted microstructure greatly influence fuel cell performance. It also implies that the ion-impregnation process can be further modified to optimize the microstructure and hence, fuel cell performance.

Conclusions

Two types of anode-supported fuel cells were fabricated by copressing and by a combination method of copressing and ion impregnation. Hydrocarbon fuels such as methane and propane were successful fuels for operating at low temperatures. For methane-fueled cells with a Ni-GDC based anode and a thin GDC electrolyte, the maximum power density achieves 519 mW/cm^2 at 600°C without carbon deposits. A novel method by applying copressing and ion impregnation was used to fabricate thin electrolyte SOFCs with Cu-GDC based anode. Because the performance of single cells fueled with C_3H_8 is dramatically lower than that fueled with CH_4 or H_2, pre-reforming of C_3H_8 (or other higher hydrocarbons) to CH_4, H_2, and CO may significantly improve fuel cell performance.

Acknowledgments

References

1. N. Q. Minh and T. Takahashi, in *Science and Technology of Ceramic Fuel Cells*, pp. 147-149, Elsevier Science B. V., Amsterdam (1994).
2. S. C. Singhal, *Solid State Ionics,* **135**, 305 (2000).
3. B. C. H. Steele, *Solid State Ionics,* **129**, 95 (2000).
4. S. de Souza, S. J. Visco, and L. C. DeJonghe, *J. Electrochem. Soc.,* **144**, L35 (1997).
5. Y. Jiang and A. V. Virkar, *J. Electrochem. Soc.,* **148**, A706 (2001).
6. C. Xia, F. Chen, and M. Liu, *Electrochem. Solid-State Lett.,* **4**, A52 (2001).
7. C. Xia and M. Liu, *Solid State Ionics,* **152**, 423 (2002).
8. S. Park, J. M. Vohs, and R. J. Gorte, *Nature (London),* **404**, 265 (2000).
9. H. Kim, S. Park, J. M. Vohs, and R. J. Gorte, *J. Electrochem. Soc.,* **148**, A693 (2001).
10. E. P. Murray, T. Tsai, and S. A. Barnett, *Nature (London),* **404**, 649 (1999).
11. C. Xia, W. Rauch, F. Chen, and M. Liu, *Solid State Ionics,* **149**, 11 (2002).
12. S. Zha, C. Xia, and G. Meng, *J. Power Sources,* **115**, 44 (2003).
13. J. Van Herle, T. Horita, T. Kawada, N. Sakai, H. Yokokawa, and M. Dokiya, *J. Am. Ceram. Soc.,* **80**, 933 (1997).
14. M. Liu, in *Ionic and Mixed Conducting Ceramics*, T. A. Ramanarayanan and H. L. Tuller, Editors, PV 91-12, p. 191, The Electrochemical Society Proceedings Series, Pennington, NJ (1991).
15. M. L. Liu and H. X. Hu, *J. Electrochem. Soc.,* **143**, L109 (1996).
16. S. Zha, W. Rauch, and M. Liu, *Solid State Ionics,* **241,** 166 (2004).
17. C. Lu, W. L. Worrell, R. J. Gorte, and J. M. Vohs, *J. Electrochem. Soc.,* **150**, A354 (2003).
18. S. Zha, Q. Fu, Y. Lang, C. Xia, and G. Meng, *Mater. Lett.,* **47**, 351 (2001).
19. J. Dong, W. Shen, and B. Tatarchuk, *Appl. Phys. Lett.,* **80**, 3733 (2002).